British Journal of Pharmacology (2003) 138, 1535–1543 © 2003 Nature Publishing Group All rights reserved 0007–1188/03 $25.00
www.nature.com/bjp

Extracellular ATP-induced calcium channel inhibition mediated by P1/P2Y purinoceptors in hamster submandibular ganglion neurons

[1]Mitsuhiro Abe, *,[1]Takayuki Endoh & [1]Takashi Suzuki

[1]Department of Physiology, Tokyo Dental College, 1-2-2, Masago, Mihama-ku, Chiba 261-8502, Japan

1 The presence and profile of purinoceptors in neurons of the hamster submandibular ganglion (SMG) have been studied using the whole-cell configuration of the patch-clamp technique.

2 Extracellular application of adenosine 5′-triphosphate (ATP) reversibly inhibited voltage-dependent Ca^{2+} channel (VDCC) currents (I_{Ca}) via $G_{i/o}$-protein in a voltage-dependent manner.

3 Extracellular application of uridine 5′-triphosphate (UTP), 2-methylthioATP (2-MeSATP), α,β-methylene ATP (α,β-MeATP) and adenosine 5′-diphosphate (ADP) also inhibited I_{Ca}. The rank order of potency was ATP = UTP > ADP > 2-MeSATP = α,β-MeATP.

4 The P2 purinoceptor antagonists, suramin and pyridoxal-5-phosphate-6-azophenyl-2′, 4′-disulfonic acid (PPADS), partially antagonized the ATP-induced inhibition of I_{Ca}, while coapplication of suramin and the P1 purinoceptor antagonist, 8-cyclopentyl-1,3-dipropylxanthine (DPCPX), virtually abolished I_{Ca} inhibition. DPCPX alone partially antagonized I_{Ca} inhibition.

5 Suramin antagonized the UTP-induced inhibition of I_{Ca}, while DPCPX had no effect.

6 Extracellular application of adenosine (ADO) also inhibited I_{Ca} in a voltage-dependent manner via $G_{i/o}$-protein activation.

7 Mainly N- and P/Q-type VDCCs were inhibited by both ATP and ADO via $G_{i/o}$-protein $\beta\gamma$ subunits in seemingly convergence pathways.

British Journal of Pharmacology (2003) **138,** 1535 – 1543. doi:10.1038/sj.bjp.0705174

Keywords: Purinergic receptor; G protein-coupled receptor superfamily; parasympathetic neuron; voltage-gated calcium channels; voltage-dependent inhibition

Abbreviations: ADO, adenosine; ADP, adenosine 5′-diphosphate; α, β-MeATP,α,β-methylene ATP; ATP, adenosine 5′-triphosphate; DPCPX, 8-cyclopentyl-1,3-dipropylxanthine; GDP-β-S, guanosine 5′-O-(2-thiodiphosphate); 2-MeSATP, 2-methylthioATP; PPADS, pyridoxal-5-phosphate-6-azophenyl-2′,4′-disulfonic acid; PTX, pertussis toxin; SMG, submandibular ganglion; UTP, uridine 5′-triphosphate; VDCC, voltage-dependent Ca^{2+} channel

Introduction

Extracellular adenosine 5′-triphosphate (ATP) is known to act as a neurotransmitter in the central and peripheral nervous systems (Burnstock, 1990; Zimmermann, 1994). It has been shown that ATP can be released, or coreleased with acetylcholine or norepinephrine, from nerve endings (Burnstock, 1990) and serves as a modulator of synaptic transmission (Ribeiro, 1996). The actions of ATP are mediated by purinoceptors that are present on many neurons. The purinoceptors are classified into two major subtypes, P1 and P2, which are preferentially activated by adenosine and ATP, respectively. P2 purinoceptors have been categorized into two major groups, P2X and P2Y, based on their pharmacological properties, as well as their molecular structure. P2X are ligand-gated ion channels, while P2Y are G-protein-coupled receptors (Burnstock, 1997).

The submandibular ganglion (SMG) neuron is a parasympathetic ganglion that receives input from preganglionic cholinergic neurons, and innervates the submandibular gland to control the secretion of saliva. This ganglion also receives input from peptidergic afferent fibers and that input provides a pathway for local reflex control of saliva secretion. Salivary glands, in particularly rat and mouse parotid glands, possess P2 purinoceptors that mediate acinar cell elevation of Ca^{2+} and amylase secretion (McMillian *et al*., 1993). In sympathetic neurons, P2Y purinoceptors have also been shown to operate on presynaptic nerve terminals to inhibit the release of a neurotransmitter (Von Kügelgen *et al*., 1993).

Recent works have demonstrated that SMG neurons possess P2X purinoceptors (Liu & Adams, 2001; Smith *et al*., 2001). In addition, as we reported in our previous study, extracellular ATP caused both depolarization and hyperpolarization of SMG neurons (Suzuki *et al*., 1990a).

Voltage-dependent Ca^{2+} channels (VDCCs) serve as crucial mediators of membrane excitability and Ca^{2+}-dependent functions such as neurotransmitter release, enzyme activity and gene expression. The modulation of VDCCs is believed to be an important means of regulating Ca^{2+} entry and thus has a direct influence on many Ca^{2+}-dependent processes. Several electrophysiological studies indicate that ATP modulates VDCCs currents (I_{Ca}) in frog sympathetic ganglia (Elmslie, 1992) and sinoatrial nodal cells (Qi & Kwan, 1996). The reported effects are quite variable: stimulatory, inhibitory or both. In SMG neurons, however, the effect of extracellular ATP on neuronal VDCCs has not yet been clarified. Therefore, the present study was conducted with the goals of (1) testing for a modulatory effect of extracellular ATP on VDCCs of SMG

*Author for correspondence; E-mail: tendoh@tdc.ac.jp

neurons, (2) determining the intracellular mechanisms in the response of extracellular ATP on VDCCs in these neurons, (3) identification of the subtype of VDCCs in the response of extracellular ATP on VDCCs in these neurons. The results indicate that both P1 and P2 purinoceptors contribute to the modulatory effect of extracellular ATP on VDCCs although adenosine only partly mimics the actions of ATP.

Methods

Cell preparation

Experiments were conducted according to international guidelines on the use of animals for experimentation. Hamster SMG neurons were acutely dissociated using a modified version of a method described previously (Yamada *et al*., 2002). In brief, male hamsters 4-to-6-weeks old were anesthetized with pentobarbital sodium (30 mg kg^{-1}, i.p.) and SMG ganglia were isolated. SMG ganglia were maintained in Ca^{2+}-free Krebs solution of the following composition (in mM): 136 NaCl, 5 KCl, 3 $MgCl_2 \cdot 6H_2O$, 10.9 glucose, 11.9 $NaHCO_3$ and 1.1 $NaH_2PO_4 \cdot 2H_2O$. SMG neurons were dissociated using collagenase type I (3 mg ml^{-1} in Ca^{2+}-free Krebs solution; Sigma) for 50 min at 37°C, followed by incubation in trypsin type I (1 mg ml^{-1} in Ca^{2+}-free Krebs solution; Sigma) for an additional 10 min. The supernatant was replaced with normal Krebs solution of the following composition (in mM): 136 NaCl, 5 KCl, 2.5 $CaCl_2$, 0.5 $MgCl_2 \cdot 6H_2O$, 10.9 glucose, 11.9 $NaHCO_3$ and 1.1 $NaH_2PO_4 \cdot 2H_2O$. Neurons were then plated onto poly-L-lysine (Sigma)-coated glass coverslips and used within 1 – 12 h.

Whole-cell patch-clamp recordings

Voltage-clamp recordings were conducted using the whole-cell configuration of the patch-clamp technique (Hamill *et al*., 1981). Recording pipettes (2 – 3 MΩ) were filled with an internal solution of the following composition (in mM): 100 CsCl, 1 $MgCl_2$, 10 HEPES, 10 BAPTA, 3.6 MgATP, 14 Tris2phosphocreatine (CP) 0.1 GTP, and 50 U ml^{-1} creatine phosphokinase (CPK). The pH was adjusted to 7.2 with CsOH. The inclusion of CP and CPK helped reduce the 'rundown' of I_{Ca}. In guanosine 5′-O-(2-thiodiphosphate) (GDP-β-S; Sigma) experiments, GTP was replaced with 0.1 mM GDP-β-S. After the formation of a giga seal, in order to record I_{Ca}, the external solution was replaced from Krebs solution to a solution containing the following (in mM): 67 choline-Cl, 100 tetraethylammonium-Cl, 5.3 KCl, 5 $CaCl_2$ and 10 HEPES. The pH was adjusted to 7.4 with Tris base. Command voltage protocols were generated using pCLAMP (version 8; Axon Instruments, Union City, CA, U.S.A.) and transformed to an analog signal using a DigiData 1200 interface (Axon Instruments, Union City, CA, U.S.A.). The command pulses were applied to cells through an L/M-EPC7 amplifier (HEKA Elektronik, Lambrecht, Germany). The currents were recorded with an L/M-EPC7 amplifier and the pCLAMP 8 acquisition system.

Materials

ATP, GDP-β-S, uridine 5′-triphosphate (UTP), 2-methylthioATP (2-MeSATP), α,β-methylene ATP (α,β-MeATP), adenosine 5′-diphosphate (ADP), suramin, 8-cyclopentyl-1,3-dipropylxanthine (DPCPX), pyridoxal-5-phosphate-6-azophenyl-2′,4′-disulphonic acid (PPADS), adenosine (ADO) and nifedipine (Nif) were purchased from Sigma. Pertussis toxin (PTX) was purchased from Calbiochem. Anti-$G_{q/11}$ antibodies were purchased from Upstate biotechnology (Lake Placid, NY, U.S.A.). The anti-$G_{q/11}$ antibodies were from rabbits immunized with a synthetic peptide corresponding to the COOH-terminal sequence of the human $G_{q/11}$ subunit. ω-conotoxin GVIA (ω-CgTx GVIA) and ω-agatoxin IVA (ω-Aga IVA) were purchased from Peptide Institute. All drugs except DPCPX and Nif were dissolved in distilled water. DPCPX and Nif were dissolved in dimethylsulfoxide (DMSO), as a stock solution at a concentration of 100 mM. All drugs were diluted to the desired final concentration in the external solution just before use. The final concentration of DMSO was $<0.01\%$, which had no effect on the I_{Ca}.

Data analysis and statistics

All data analyses were performed using the pCLAMP 8.0 acquisition system. Values in text and figures are expressed as mean ± s.e.m. Statistical analysis was made by Student's *t*-test for comparisons between pairs of groups and by one-way analysis of variance (ANOVA) followed by Dunnett's test. Probability (P) values of less than 0.05 were considered significant.

Results

Extracellular ATP-induced inhibition of I_{Ca}

An example of ATP-induced inhibition of I_{Ca} is shown in Figure 1. To investigate the voltage dependency of inhibition of I_{Ca} by ATP, we used a double-pulse voltage protocol as shown in Figure 1a (left). In this and in subsequent descriptions, we referred to I_{Ca} before and after the strong depolarizing voltage pulse as 'I_{Ca} (−prepulse)' and 'I_{Ca} (+prepulse)', respectively. Application of 100 μM ATP inhibited I_{Ca} (−prepulse) from −2307.5 to −937.5 pA (59.3% inhibition) in this neuron. On the other hand, 100 μM ATP inhibited I_{Ca} (+prepulse) from −2710 to −1962.5 pA (27.5% inhibition) in the same neuron. On average, the inhibition of I_{Ca} was 42.0 ± 4.6% for I_{Ca} (−prepulse) and 20.4 ± 2.4% for I_{Ca} (+prepulse) ($n=8$). These results suggest that the application of a strong depolarizing voltage prepulse attenuated the ATP-induced inhibition of I_{Ca}. Note that a strong depolarizing voltage pulse alone increased the amplitude of the I_{Ca} in these neurons (e.g. Figure 1a), suggesting that tonic inhibition (Dolphin, 1998) was present before application of the agonists to SMG neurons.

An example of the current – voltage relations before and after application of 100 μM ATP is shown in Figure 1b. From a holding potential of −80 mV, the I_{Ca} was activated after −40 mV with a peak current amplitude at −10 mV. ATP-induced inhibition resulted in a shift in the voltage dependence of the I_{Ca} to more positive potentials. Similar observations were made for UTP-induced inhibition of I_{Ca} mediated by expressed $P2Y_2$ receptors in sympathetic neurons (Filippov *et al*., 1998).

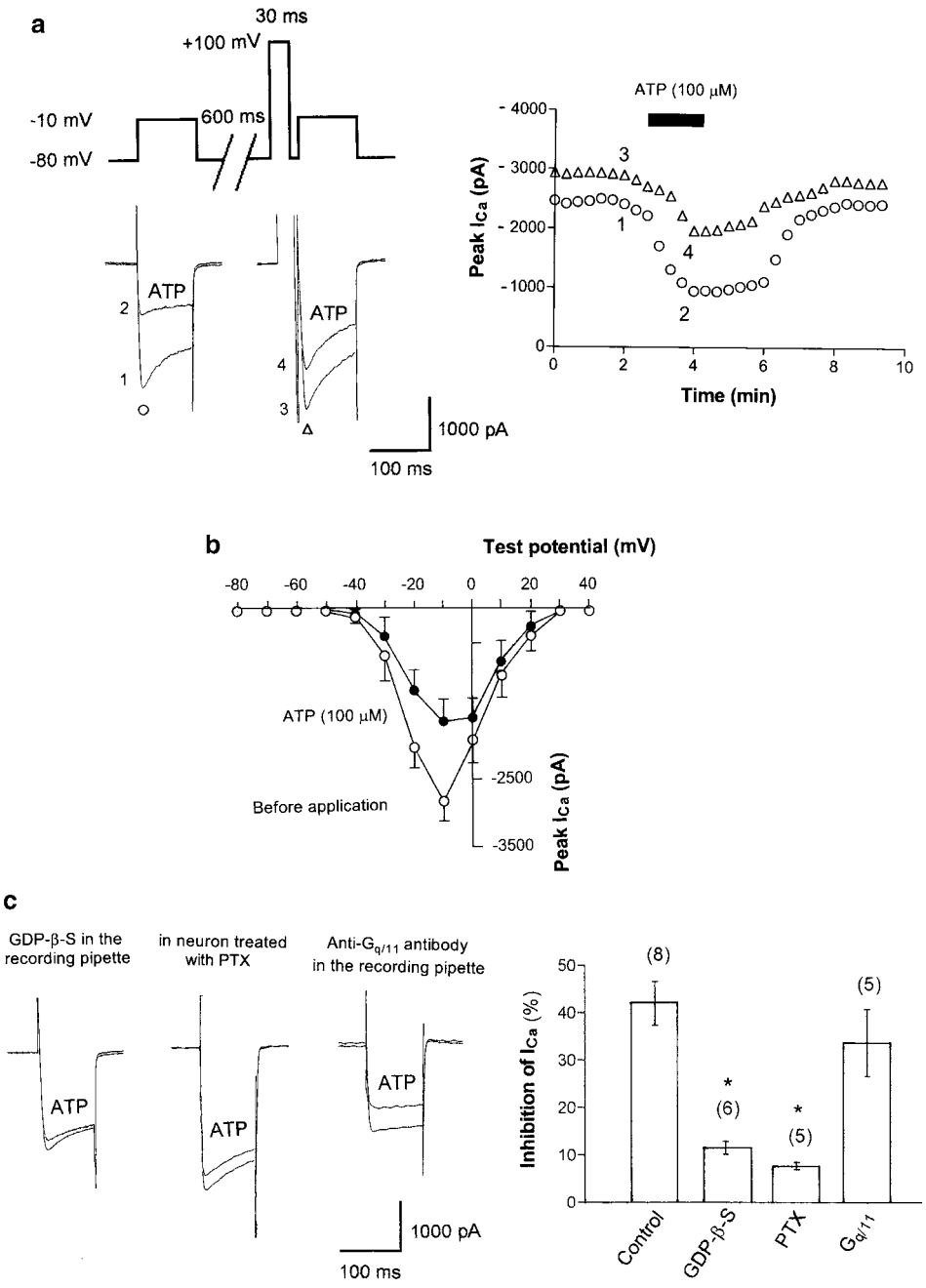

Figure 1 Extracellular ATP-induced inhibition of I_{Ca}. (a) Left panel: Typical superimposed I_{Ca} traces recorded using a double-pulse voltage protocol at the times indicated in the time course graph (right panel). Paired I_{Ca} were evoked from a holding potential of −80 mV by a 100 ms voltage step to −10 mV at 20 s intervals. An intervening strong depolarizing prepulse (100 mV, 30 ms) ended 5 ms prior to the second I_{Ca} activation. Right panel: typical time course of ATP-induced I_{Ca} inhibition. Opened circle and triangles in the graph indicate I_{Ca} (−prepulse) and I_{Ca} (+prepulse), respectively. ATP (100 μM) was bath applied during the time indicated by the filled bar. (b) Current – voltage relations of I_{Ca} evoked by a series of voltage steps from a holding potential of −80 mV to test pulses between −80 mV and +40 mV in +10 mV increments) in the absence (opened points) and presence (filled points) of 100 μM ATP. Values of I_{Ca} are the averages of five neurons. (c) Extracellular ATP-induced inhibition of I_{Ca} in the presence of G-protein blocker. Left panel: typical superimposed I_{Ca} traces recorded in the presence of GDP-β-S (0.1 mM for 7 min) contained in the recording pipette. Center panel: typical superimposed I_{Ca} traces in neuron treated with $G_{i/o}$-protein blocker, PTX (500 ng ml^{-1} for 12 h at 37°C). Right panel: typical superimposed I_{Ca} traces recorded in the presence of anti-$G_{q/11}$ antibody contained in the recording pipette (0.5 mg ml^{-1} for 7 min). Right graph: summary of ATP-induced inhibition of I_{Ca} in various conditions. The histogram demonstrates the degree of I_{Ca} inhibition by 100 μM ATP in control (recording pipette was filled with GTP), intracellular dialysis with GDP-β-S, after PTX and intracellular dialysis with anti-$G_{q/11}$ antibody. Numbers in parentheses indicate the number of neurons tested. *$P<0.005$ compared with control.

Extracellular ATP-induced inhibition of I_{Ca} mediated by P2Y purinoceptors

In the next series of experiments, we investigated whether or not G-protein is involved in the extracellular ATP-induced inhibition of I_{Ca}. Experiments were performed using a recording pipette filled with an internal solution containing GDP-β-S (0.1 mM), a nonhydrolyzable analog of GDP and a competitive inhibitor of G-proteins. In each experiment, the tip of the recording pipette was filled with the standard internal solution (see above), and the pipette was then backfilled with a solution substituted for GDP-β-S. An example of the effect of 100 μM ATP on I_{Ca} recorded in the presence of GDP-β-S in the pipette solution is shown in Figure 1c (left). As summarized in Figure 1c, GDP-β-S in the pipette solution attenuated the ATP-induced inhibition of I_{Ca}. These results suggest that a G-protein is indeed involved in the ATP-induced inhibition of I_{Ca} in SMG neurons.

G-proteins are heterotrimeric molecules with α,β and γ subunits. The α subunits can be classified into families, depending on whether they are targets for PTX ($G_{i/o}$), cholera toxin (G_s) or neither. Numerous studies demonstrated that long (12 – 24 h) incubations in PTX can be used to inactivate G-proteins of the G_i and G_o classes. To characterize the G-protein subtypes in ATP-induced inhibition of I_{Ca}, we verified whether the effect of ATP was mediated via G_i- or G_o-proteins. An example of the effect of ATP on I_{Ca} in a neuron treated with PTX (500 ng ml^{-1} for 12 h at 37°C) is shown in Figure 1c (centre). As summarized in Figure 1c, pretreatment of PTX attenuated the ATP-induced inhibition of I_{Ca}.

The contribution of $G_{q/11}$-proteins in the ATP-induced inhibition of I_{Ca} was next examined. Experiments were performed with pipette solutions containing anti-$G_{q/11}$ antibody. In these experiments, anti-$G_{q/11}$ antibody (1 : 50 dilution; final concentration, approximately 0.5 mg ml^{-1}) was dissolved in the internal solution. In this experiment, the tip of the recording pipette was filled with the standard internal solution, and the pipette was then backfilled with the solution containing anti-$G_{q/11}$ antibody. An example of the effect of ATP on I_{Ca} in the presence of anti-$G_{q/11}$ antibody in the pipette solution is shown in Figure 1c (right). As summarized in Figure 1c, anti-$G_{q/11}$ antibody in the pipette solution did not attenuate the ATP-induced inhibition of I_{Ca}.

These results suggest that the $G_{i/o}$-protein is involved in the ATP-induced inhibition of I_{Ca} but not $G_{q/11}$-protein in SMG neurons. As shown in Figure 1c, with GDP-β-S and anti-$G_{q/11}$ antibody in the recording pipette, basal I_{Ca} (before application of ATP or ADO) is smaller than that under control condition (GTP in the recording pipette). In this study, applications of ATP or ADP were started 7 min after formation of the whole-cell configuration to obtain the requisite intracellular dialysis of the compounds. Therefore, it was not clear if GDP-β-S and anti-$G_{q/11}$ antibody in the recording pipette caused 'rundown' or reduction of basal I_{Ca}. On the other hand, application of PTX did not alter the basal I_{Ca} (Figure 1c).

Pharmacological characterization of extracellular ATP-induced inhibition of I_{Ca} mediated by P2Y purinoceptors

Since ATP is a nonselective purinoceptor agonist, we have further characterized the pharmacological features of the P2Y purinoceptor-induced inhibition of I_{Ca} in SMG neurons. Application of 100 μM UTP inhibited I_{Ca} from −2447.5 to −1407.5 pA (42.2% inhibition) in this neuron (Figure 2a). Application of 100 μM 2-MeSATP also inhibited I_{Ca} from −2167.5 to −1955 pA (9.8% inhibition) in this neuron (Figure 2a). Application of 100 μM α,β-MeATP inhibited I_{Ca} from −1997.5 to −1710 pA (14.3% inhibition) in this neuron

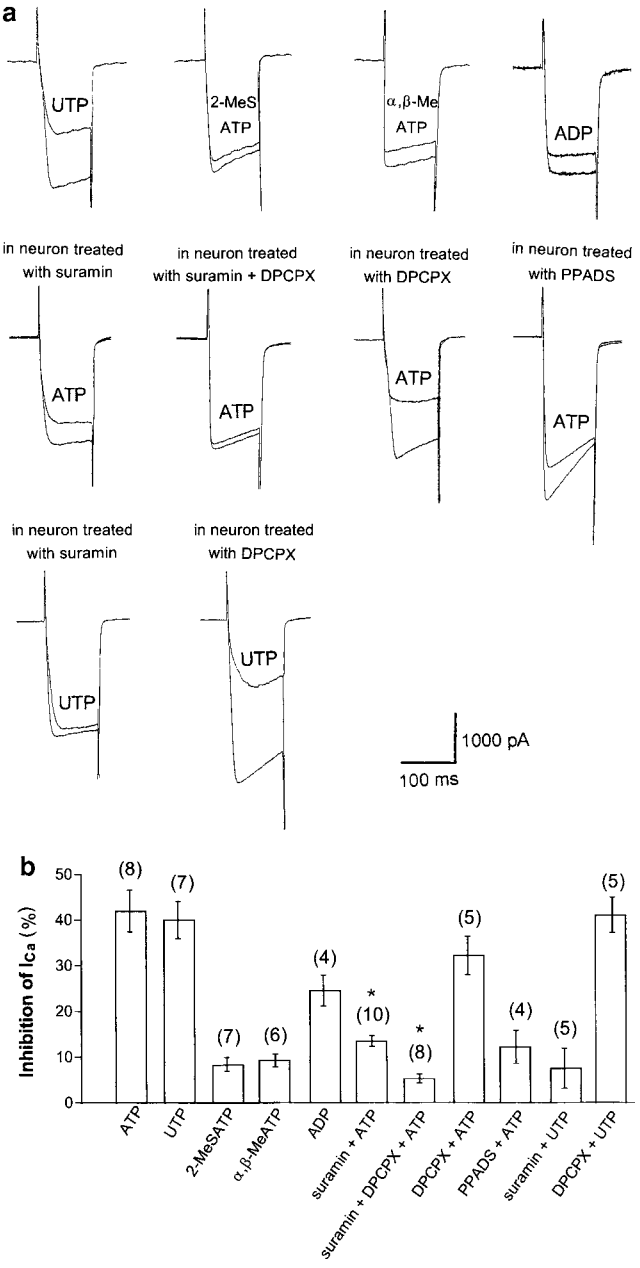

Figure 2 Extracellular ATP- and ATP-analog-induced inhibition of I_{Ca} in various conditions. (a) Upper panel: typical superimposed I_{Ca} traces in the absence and presence of 100 μM UTP, 2-MeSATP, α,β-MeATP and ADP. Center panel: typical superimposed I_{Ca} traces in the absence and presence of 100 μM ATP with various antagonists. Lower panel: typical superimposed I_{Ca} traces in the absence and presence of 100 μM UTP with various antagonists. (b) Summary of ATP- and ATP-analog-induced inhibition of I_{Ca} in various conditions. The histogram demonstrates the degree of I_{Ca} inhibition by various agonists and various conditions at the concentration of 100 μM. Numbers in parentheses indicate the number of neurons tested. *$P<0.005$ compared with control.

(Figure 2a). Application of 100 μM ADP inhibited I_{Ca} from -2061 to -1717.5 pA (16.6% inhibition) in this neuron (Figure 2a).

Contribution of P1 and P2 purinoceptors to ATP-induced inhibition of I_{Ca}

To confirm whether the ATP-induced inhibitory effect was mediated by P2 purinoceptors, we used suramin which is an antagonist for the P2 purinoceptors. As shown in Figure 2a and b, a high concentration of suramin (100 μM) did not completely antagonize ATP-induced inhibition of I_{Ca} in SMG neurons (42.0$\pm$4.6% for ATP only and 13.5$\pm$1.2% for ATP in neuron treated with suramin, $n=8$ and 10, respectively). These results suggest that the ATP-induced inhibition of I_{Ca} is mediated not only by P2Y but also other receptors, possibly P1 purinoceptors in SMG neurons. Therefore, we next investigated the effects of ATP on I_{Ca} in the presence of a P1 purinoceptor antagonist, DPCPX. An example of ATP-induced inhibition of I_{Ca} in the presence of both suramin (100 μM) and DPCPX (1 μM) is shown in Figure 2a. Suramin (100 μM) and DPCPX virtually abolished ATP-induced inhibition of I_{Ca} (42.0$\pm$4.6% for ATP only and 5.3$\pm$1.0% for ATP in neuron treated with suramin + DPCPX, $n=8$). DPCPX alone partially antagonized ATP-induced inhibition of I_{Ca} (32.2$\pm$4.2% for ATP in neuron treated with DPCPX, $n=5$). PPADS also partially antagonized ATP-induced inhibition of I_{Ca} (12.2$\pm$3.6% for ATP in neuron treated with PPADS, $n=4$). These results indicate that both P1 and P2 purinoceptors contribute to the ATP-induced inhibition of I_{Ca} in SMG neurons.

Furthermore, we investigated the effects of purinoceptor antagonists on UTP-induced inhibition of I_{Ca}. As shown in Figure 2a and b, suramin (100 μM) completely antagonized UTP-induced inhibition of I_{Ca}, whereas DPCPX (1 μM) failed to affect UTP-induced inhibition of I_{Ca} (40.0$\pm$4.1% for UTP only, 7.5$\pm$4.4% for UTP in neuron treated with suramin and 41.1$\pm$3.9% for UTP in neuron treated with DPCPX, $n=7$, 5 and 5, respectively).

Extracellular adenosine-induced inhibition of I_{Ca}

We next investigated the effects of ADO on I_{Ca}. An example of ADO-induced inhibition of I_{Ca} is shown in Figure 3a, where application of a strong depolarizing voltage prepulse attenuated the ADO-induced inhibition of I_{Ca}.

To confirm whether a G-protein is involved in the extracellular ADO-induced inhibition of I_{Ca}, experiments were again performed using a recording pipette filled with the internal solution containing GDP-β-S. An example of the effect of 1 μM ADO on I_{Ca} recorded in the presence of GDP-β-S in the pipette solution is shown in Figure 3b (left). As summarized in Figure 3b, GDP-β-S in the pipette solution attenuated the ADO-induced inhibition of I_{Ca}.

To characterize the G-protein subtype in ADO-induced inhibition of I_{Ca}, we also verified whether the effect of ADO was mediated via G_i- or G_o-proteins. An example of the effect of ADO on I_{Ca} in neuron treated with PTX (500 ng ml^{-1} for 12 h at 37°C) is given in the figure. As summarized in Figure 3b (center), pretreatment of PTX attenuated the ADO-induced inhibition of I_{Ca}.

The potential contribution of $G_{q/11}$-proteins in the ADO-induced inhibition of I_{Ca} was next examined. An example of the effect of ADO on I_{Ca} in the presence of anti-$G_{q/11}$ antibody in the pipette solution is shown in Figure 3b (right). The anti-$G_{q/11}$ antibody in the pipette solution did not attenuate the ADO-induced inhibition of I_{Ca}. These combined results suggest that a $G_{i/o}$-protein and not $G_{q/11}$-protein is involved in the ADO-induced inhibition of I_{Ca} in SMG neurons.

The dose – response relations in the ATP-, UTP-, ADP- and ADO-induced inhibition of I_{Ca} are also shown in Figure 3c. The half-maximum inhibitory concentrations (IC_{50}) of ATP and UTP were estimated to be 79.5 and 78.0 μM, respectively. The IC_{50} of ADO was estimated to be 985 nM. The rank order of potency of P2 purinoceptor agonists was ATP = UTP > ADP > 2-MeSATP = α,β-MeATP.

Pharmacological characterization of VDCC subtypes inhibited by P2Y and P1 purinoceptors

On the basis of pharmacological properties, VDCCs can be separated into low-voltage activated type (T-type) and high-voltage activated types (L-, N-, P/Q- and R-types). We have shown that SMG neurons possess several types of VDCCs (Endoh & Suzuki, 1998), that is, dihydropyridine-sensitive component ($I_{Ca\text{-}L}$), ω-CgTx GVIA-sensitive component ($I_{Ca\text{-}N}$) and ω-Aga IVA-sensitive component ($I_{Ca\text{-}P/Q}$). Mean percentages of $I_{Ca\text{-}L}$, $I_{Ca\text{-}N}$ and $I_{Ca\text{-}P/Q}$ of total I_{Ca} were 48.0, 36.1 and 13.5%, respectively. Therefore, we next attempted to identify which types of the VDCCs are inhibited by extracellular ATP. Since the contribution of the R-type VDCCs to the total I_{Ca} is marginal (mean percentage of $I_{Ca\text{-}R}$ was 3.6%), we investigated the effects of ATP on the L-, N- and P/Q-type I_{Ca} components.

The effect of ATP on the $I_{Ca\text{-}L}$ was investigated using neurons treated with ω-CgTx GVIA (1 μM, N-type VDCC blocker) and ω-Aga IVA (1 μM, P/Q-type VDCC blocker) (Figure 4a, upper trace). The effect of ATP on the $I_{Ca\text{-}N}$ was investigated using neurons treated with nifedipine (10 μM, Nif; L-type VDCC blocker) and ω-Aga IVA (1 μM) (Figure 4a, middle trace). The effect of ATP on the $I_{Ca\text{-}P/Q}$ was investigated using neurons treated with Nif (10 μM) and ω-CgTx GVIA (1 μM) (Figure 4a, lower trace). The inhibition of $I_{Ca\text{-}L}$, $I_{Ca\text{-}N}$ and $I_{Ca\text{-}P/Q}$ components by extracellular ATP was 4.6$\pm$0.5, 15.8$\pm$1.3 and 5.3$\pm$0.8%, respectively, of the total I_{Ca}. Only the inhibition of $I_{Ca\text{-}N}$ and $I_{Ca\text{-}P/Q}$ was significant. Results shown in Figure 4a demonstrate clearly that ATP inhibited N- and P/Q-type I_{Ca} components in SMG neurons.

As shown in Figure 3, 100 M ATP inhibited I_{Ca} by 42.0$\pm$4.6% ($n=8$). However, the accumulative degree of ATP-induced inhibition of I_{Ca} was about 25% in Figure 4, because extracellular application of VDCC blockers required too much time for the full ATP effects to appear. Thus, it was difficult to prevent rundown, even though we had added CP and CPK in the recording pipette.

We next investigated the effects of ADO on the L-, N- and P/Q-type I_{Ca} components. The inhibition of $I_{Ca\text{-}L}$, $I_{Ca\text{-}N}$ and $I_{Ca\text{-}P/Q}$ components by extracellular ADO was 7.1$\pm$1.1, 15.1$\pm$2.2, and 5.0$\pm$1.6%, respectively, of the total I_{Ca}. Only the inhibition of $I_{Ca\text{-}N}$ and $I_{Ca\text{-}P/Q}$ was significant. Results shown in Figure 4b demonstrate clearly that ADO inhibited N- and P/Q-type I_{Ca} components in SMG neurons.

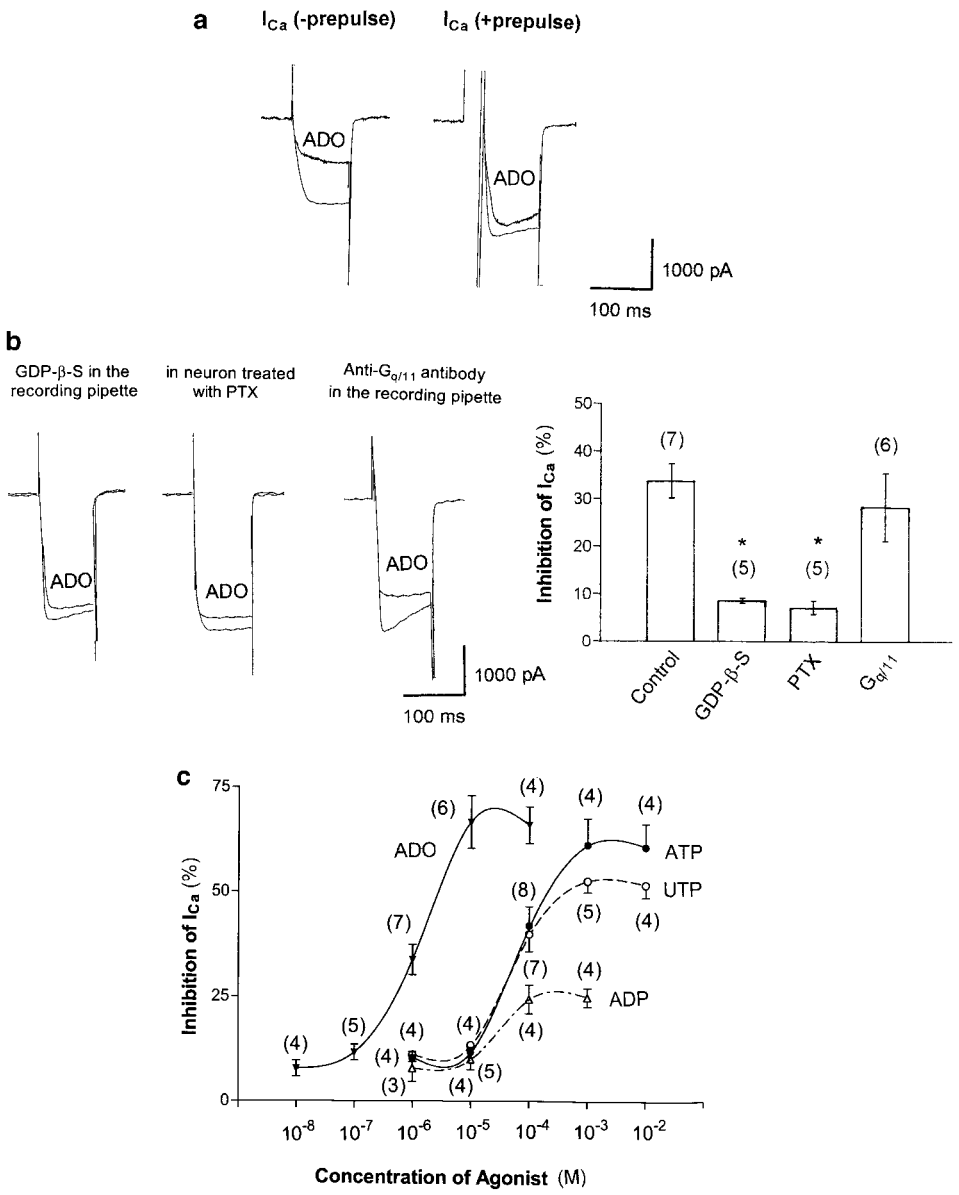

Figure 3 Extracellular ADO-induced inhibition of I_{Ca}. (a) Typical superimposed I_{Ca} traces recorded using a double-pulse voltage protocol in the absence and presence of 1 μM ADO. (b) Extracellular ADO-induced inhibition of I_{Ca} in the presence of G-protein blocker. Left panel: typical superimposed I_{Ca} traces recorded in the presence of GDP-β-S (0.1 mM for 7 min) contained in the recording pipette. Center panel: typical superimposed I_{Ca} traces in neuron treated with $G_{i/o}$-protein blocker, PTX (500 ng ml^{-1} for 12 h at 37°C). Right panel: typical superimposed I_{Ca} traces recorded in the presence of anti-$G_{q/11}$ antibody contained in the recording pipette (0.5 mg ml^{-1} for 7 min). Right graph: summary of ATP-induced inhibition of I_{Ca} in various conditions. The histogram demonstrates the degree of I_{Ca} inhibition by 100 μM ATP in control (recording pipette was filled with GTP), intracellular dialysis with GDP-β-S after PTX and intracellular dialysis with anti-$G_{q/11}$ antibody. Numbers in parentheses indicate the number of neurons tested. *$P<0.0005$ compared with control. (c) Dose dependence of ATP-, UTP-, ADP- and ADO-induced inhibition of I_{Ca}. Numbers in parentheses indicate the number of neurons tested.

Convergence of P1 and P2Y purinoceptor signalling to inhibit I_{Ca}

Convergence or nonadditivity between P1 and P2Y purinoceptor inhibitory pathways was investigated by the coapplication of agonists and by comparing the inhibition of the I_{Ca} with that produced by each of these agonists alone. A volume of 100 μM ATP inhibited I_{Ca} by 42.0$\pm$4.6% ($n=8$), 1 μM ADO inhibited I_{Ca} by 33.8$\pm$3.6% ($n=7$), and the coapplication of both 100 μM ATP and 1 μM ADO inhibited I_{Ca} by 33.9$\pm$4.2% ($n=5$). Thus, the mean inhibition of I_{Ca} induced by ATP was unaltered by its coapplication with ADO, suggesting that the actions of ATP and ADO are not additive, and further suggesting convergence in these inhibitory pathways (Figure 5).

Discussion

In this study, we have demonstrated that P1 and P2Y purinoceptors are coexpressed postsynaptically in SMG neurons. Both P1 and P2Y purinoceptors inhibit N- and P/Q-type VDCCs, presumably via G $\beta\gamma$ subunits by extracellular

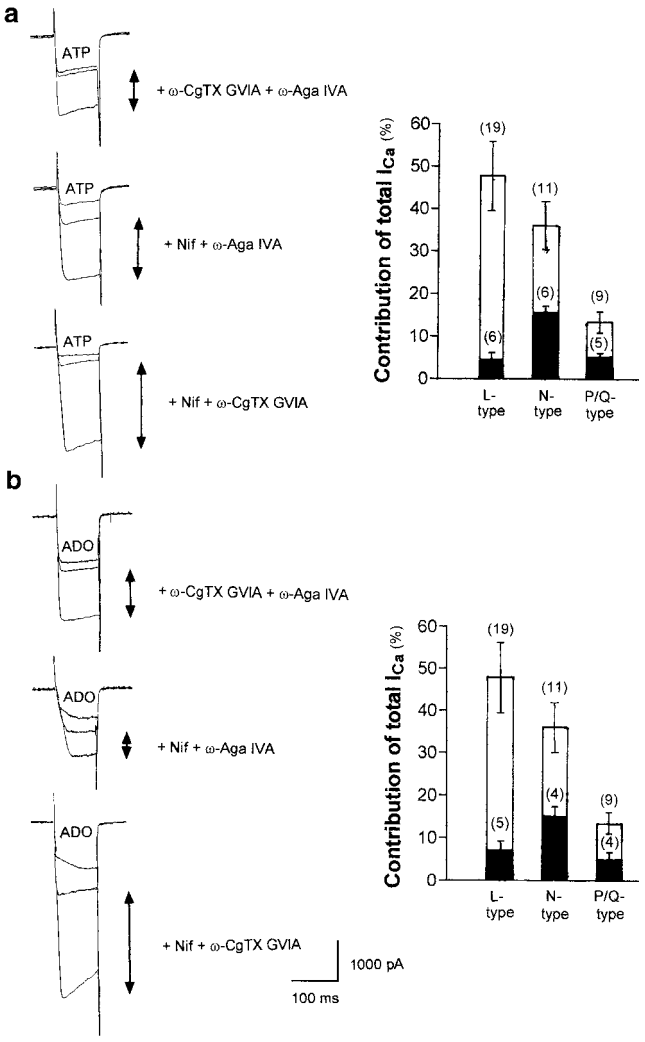

Figure 4 Extracellular ATP- and ADO-induced inhibition of distinct I_{Ca}. (a) Upper panel: effect of ATP on $I_{Ca\text{-}L}$. Center panel: effect of ATP on $I_{Ca\text{-}N}$. Lower panel: effect of ATP on $I_{Ca\text{-}P/Q}$. Right panel: fractional components of L-, N- and P/Q-types of I_{Ca} and those inhibited by 100 μM ATP. (b) Upper panel: effect of ADO on $I_{Ca\text{-}L}$. Center panel: effect of ADO on $I_{Ca\text{-}N}$. Lower panel: Effect of ADO on $I_{Ca\text{-}P/Q}$. Right panel: fractional components of L-, N- and P/Q-types of I_{Ca} and those inhibited by 1 μM ADO.

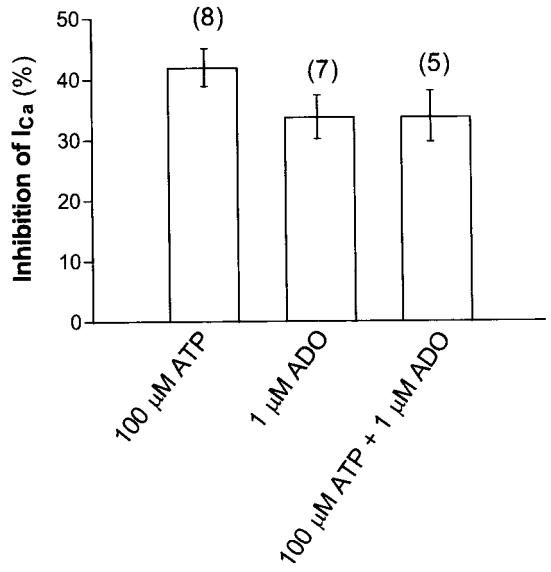

Figure 5 Extracellular ATP- and ADO-induced inhibition of I_{Ca}. Summary of ATP- and ADO-induced inhibition of I_{Ca}. The histogram demonstrates the degree of I_{Ca} inhibition by 100 μM ATP alone, 1 μM ADO alone and coapplication of 100 μM ATP and 1 μM ADO.

ATP. Our present results, together with the results that P2X purinoceptors are also located on SMG neurons (Liu & Adams, 2001; Smith *et al*., 2001), indicate the growing importance of purinoceptors in the regulation of this ganglion.

According to biophysical criteria, the inhibitory effects of modulation of I_{Ca} can be divided into voltage-dependent (VD) and voltage-independent (VI) mechanisms. The VD mechanism is relieved at a higher potential or by means of a strong depolarizing voltage prepulse to positive voltages (Bean, 1989; Dolphin, 1996, 1998), whereas the VI mechanism is not affected by a strong voltage depolarizing prepulse (Formenti *et al*., 1993). In frog sympathetic ganglion cells, ATP inhibits I_{Ca} in a VD mechanism (Elmslie, 1992). In contrast, in chromaffin cells, ATP inhibits I_{Ca} in a VI mechanism (Hernández-Guijo *et al*., 1999).

In our experiments, double-pulse protocols demonstrated that inhibition of I_{Ca} produced by ATP was greatly reduced after a 100 mV depolarizing prepulse and therefore a VD mechanism. The prepulse also abolished the slowing of the current onset produced by ATP. A similar effect was reported for the modulation of I_{Ca} by endogenous GABA receptors in sensory neurons (Grassi & Lux, 1989). Slowing of the current onset by ATP in neurons also indicated that ATP-induced inhibition of I_{Ca} was in VD mechanism and relieved during depolarization (Bean, 1989), as reported previously for other G-protein-coupled receptors. In addition, the current – voltage relation of I_{Ca} shows that the peak current – voltage relation was altered by ATP. Similar observations were made for superior cervical sympathetic neurons (Filippov *et al*., 1998). The VD manner inhibition is mediated by direct binding of the G-protein $\beta\gamma$ subunits to the VDCCs in a membrane-delimited manner (Herlitze *et al*., 1996; Ikeda, 1996). Our results also indicate that $G_{i/o}$-protein is involved in the ATP- and ADO-induced inhibition of I_{Ca}. It was demonstrated that $G_{i/o}$-protein is involved in the ATP-induced inhibition of I_{Ca} in bovine chromaffin cells (Gandía *et al*., 1993). In contrast, $G_{i/o}$-protein is not involved in the ATP-induced inhibition of I_{Ca} in frog sympathetic ganglion (Elmslie, 1992). In supraoptic neurons, $G_{i/o}$-protein is involved in the ADO-induced inhibition of I_{Ca} (Noguchi & Yamashita, 2000).

Purinoceptors are classified into P2 purinoceptors, sensitive to ATP and ADP, and P1 purinoceptors responding to AMP and ADO. In the present study, suramin partially antagonized the ATP-induced inhibition of I_{Ca}, while coapplication of DPCPX and suramin nearly completely antagonized it in SMG neurons suggesting the presence of both P1 and P2 purinoceptor subtypes. It has been reported that ectoenzymes are located on the cell membrane which can efficiently breakdown the ATP to ADO (Welford *et al*., 1986). Our data indicate that not only P2Y but also P1 purinoceptors contributed to the ATP-induced inhibition of I_{Ca} in SMG neurons. It has already been reported that P1 purinoceptors

inhibit I_{Ca} (Alvarez *et al*., 1990; Kato *et al*., 1990). We have also reported that application of ADO caused pivotal responses in SMG neurons (Suzuki *et al*., 1990b). In the present study, our data indicated that the extracellular ADO inhibited N- and P/Q-type VDCCs mediated by P1 purinoceptors in SMG neurons.

Cloning and pharmacological studies revealed at least five distinct subtypes of P2Y purinoceptors: $P2Y_1$, $P2Y_2$, $P2Y_4$, $P2Y_6$ and $P2Y_{11}$ (Boarder & Hourani, 1998). In addition, the localization and pharmacological profiles of subtypes of the P2Y family are further reported (Burnstock, 1997). The $P2Y_2$, $P2Y_4$ and $P2Y_6$ purinoceptor subtypes have been shown to be responsive to UTP (Lustig *et al*., 1993; Bogdanov *et al*., 1998; Ralevic & Burnstock, 1998; Filippov *et al*., 1999). The $P2Y_2$ and $P2Y_4$ purinoceptors are equipotently activated by ATP and UTP (Lustig *et al*., 1993; Bogdanov *et al*., 1998; Ralevic and Burnstock, 1998). ATP was shown to be practically inactive at the $P2Y_6$ purinoceptor in rat sympathetic neurons, whereas UTP can be its effective agonist (Filippov *et al*., 1999). The $P2Y_1$ purinoceptor's rank order of potency is as follows: 2-MeSATP > ATP > UTP. The $P2Y_2$ purinoceptor's rank order of potency is as follows: ATP = UTP $\gg$ 2MeSATP. The $P2Y_4$ purinoceptor's rank order of potency is as follows: UTP > ATP = ADP. The $P2Y_6$ purinoceptor's rank order of potency is as follows: UTP > 2MeSATP > ATP. The $P2Y_{11}$ purinoceptor's rank order of potency is as follows: ATP > 2-MeSATP $\gg$ UTP (Burnstock, 1997). In addition, suramin antagonizes $P2Y_2$ purinoceptors, but both $P2Y_4$ and $P2Y_6$ purinoceptors are suramin-insensitive (Boarder & Hourani, 1998; Bogdanov *et al*., 1998; King *et al*., 1998; Ralevic & Burnstock, 1998). On the other hand, PPADS are reported to antagonize $P2Y_2$, $P2Y_4$ and $P2Y_6$ purinoceptors (Robaye *et al*., 1997; Bogdanov *et al*., 1998). Therefore, we consider that $P2Y_2$ is the most possible candidate of P2Y purinoceptor subtype in P2Y-induced inhibition of I_{Ca} in SMG neurons.

Amino-acid sequence and pharmacological studies revealed four distinct subtypes of P1 purinoceptors: A_1, A_{2a}, A_{2b} and A_3 (Fredholm *et al*., 1994; Ralevic & Burnstock, 1998). DPDPX is a specific antagonist of A_1 purinoceptor. Thus, we consider that A_1 is the most possible candidate of P1 purinoceptor subtype in P1-induced inhibition of I_{Ca} in SMG neurons. It will be important in future experiments to determine which types of P1 purinoceptors contribute to the P1-induced inhibition of I_{Ca} in SMG neurons.

ATP- and UTP-induced inhibition of I_{Ca} was concentration dependent, IC_{50} of ATP and UTP being 79.5 μM and 78.0 M, respectively. The IC_{50} of ATP obtained here (79.5 μM) was similar to that found in other cell types (100 μM in sinoatrial nodal cell, Qi & Kwan, 1996; 55 μM in pelvic ganglion neurons, Zhong *et al*., 2001).

VDCCs are heteromultimers composed of a pore-forming α1 subunit and several auxiliary subunits (Jones, 1998). In the mammalian nervous system, five α1 subunits that exhibit distinct cellular and subcellular distributions have been described. Functional studies indicate that α1C and α1D subunits encode L-type VDCCs (Williams *et al*., 1992a; Tomlinson *et al*., 1993), α1B subunit encodes N-type VDCCs (Williams *et al*., 1992b; Stea *et al*., 1993), α1A subunit encodes VDCCs with some properties similar to both P- and Q-types (Sather *et al*., 1993; Stea *et al*., 1994) and α1E subunit encodes R-type VDCCs (Soong *et al*., 1993). Many neurotransmitter-induced inhibition of VDCCs is produced by the G $\beta\gamma$ dimers, which associate with α1B VDCCs in particular (Herlitze *et al*., 1996; Ikeda, 1996) (but also with α1A and α1E), in a membrane-delimited manner. The relatively few inhibitory effects of L-type I_{Ca} component in this study are in agreement with the fact that G $\beta\gamma$ dimers cannot bind to either the I – II linker region of L-type α1C subunit (De Waard *et al*., 1997) or the carboxyl terminus of α1C (Qin *et al*., 1997).

References

ALVAREZ, T.L., MONGO, K., SCAMPS, F. & VASSORT, G. (1990). Effects of purinergic stimulation on Ca current in single frog cardiac cells. *Pflügers Arch. Eur. J. Physiol.,* **416,** 189 – 195.

BEAN, B.P. (1989). Neurotransmitter inhibition of neuronal calcium currents by changes in channel voltage dependence. *Nature,* **340,** 153 – 156.

BOARDER, M.R. & HOURANI, S.M.O. (1998). The regulation of vascular function by P2 receptors: multiple sites and multiple receptors. *Trends Pharmacol. Sci.,* **19,** 99 – 107.

BOGDANOV, Y.D., WILDMAN, S.S., CLEMENTS, M.P., KING, B.F. & BURNSTOCK, G. (1998). Molecular cloning and characterization of rat $P2Y_4$ nucleotide receptor. *Br. J. Pharmacol.,* **124,** 428 – 439.

BURNSTOCK, G. (1990). Overview. Purinergic mechanisms. *Ann. N. Y. Acad. Sci.,* **603,** 1 – 17.

BURNSTOCK, G. (1997). The past, present and future of purine nucleotides as signalling molecules. *Neuropharmacology,* **36,** 1127 – 1139.

DE WAARD, M., LIU, H.Y., WALKER, D., SCOTT, V.E.S., GUNETT, C.A. & CAMPBELL, K.P. (1997). Direct binding of G-protein $\beta\gamma$ complex to voltage-dependent calcium channels. *Nature,* **385,** 446 – 450.

DOLPHIN, A.C. (1996). Facilitation of Ca^{2+} current in excitable cells. *Trends Neurosci.,* **19,** 35 – 43.

DOLPHIN, A.C. (1998). Mechanisms of modulation of voltage-dependent calcium channels by G-proteins. *J. Physiol.,* **506,** 3 – 11.

ELMSLIE, K.S. (1992). Calcium current modulation in frog sympathetic neurones: multiple neurotransmitters and G proteins. *J. Physiol.,* **451,** 229 – 246.

ENDOH, T. & SUZUKI, T. (1998). The regulating manner of opioid receptors on distinct types of calcium channels in hamster submandibular ganglion cells. *Arch. Oral Biol.,* **43,** 221 – 233.

FILIPPOV, A.K., WEBB, T.E., BARNARD, E.A. & BROWN, D.A. (1998). $P2Y_2$ nucleotide receptors expressed heterologously in sympathetic neurons inhibit both N-type Ca^{2+} and M-type K^+ currents. *J. Neurosci.,* **18,** 5170 – 5179.

FILIPPOV, A.K., WEBB, T.E., BARNARD, E.A. & BROWN, D.A. (1999). Dual coupling of heterologously-expressed rat $P2Y_6$ nucleotide receptors to N-type Ca^{2+} and M-type K^+ currents in rat sympathetic neurones. *Br. J. Pharmacol.,* **126,** 1009 – 1017.

FORMENTI, A., ARRIGONI, E. & MANCIA, M. (1993). Two distinct modulatory effects on calcium channels in adult rat sensory neurons. *Biophys. J.,* **64,** 1029 – 1037.

FREDHOLM, B.B., ABBRACCHIO, M.P., BURNSTOCK, G., DALY, J.W., HARDEN, T.K., JACOBSON, K.A., LEFF, P. & WILLIAMS, M. (1994). Nomenclature and classification of purinoceptors. *Pharmacol. Rev.,* **46,** 143 – 156.

GANDÍA, L., GARCÍA, A.G. & MORAD, M. (1993). ATP modulation of calcium channels in chromaffin cells. *J. Physiol.,* **470,** 55 – 72.

GRASSI, F. & LUX, H.D. (1989). Voltage-dependence GABA-induced modulation of in chick sensory neurons. *Neurosci. Lett.,* **105,** 113 – 119.

HAMILL, O.P., MARTY, A., NEHER, E., SAKMANN, B. & SIGWORTH, F.J. (1981). Improved patch-clamp techniques for high-resolution current recording from cells and cell-free membrane patches. *Pflügers Arch. Eur. J. Physiol.,* **391,** 85 – 100.

HERLITZE, S., GARCIA, D.E., MACKIE, K., HILLE, B., SCHEUER, T. & CATTERALL, W.A. (1996). Modulation of Ca^{2+} channels by G-protein $\beta\gamma$ subunits. *Nature,* **380,** 258 – 262.

HERNÁNDEZ-GUIJO, J.M., CARABELLI, V., GANDÍA, L., GARCÍA, A.G. & CARBONE, E. (1999). Voltage-independent autocrine modulation of L-type channels mediated by ATP, opioids and catecholamines in rat chromaffin cells. *Eur. J. Neurosci.,* **11,** 3574 – 3584.

IKEDA, S.R. (1996). Voltage-dependent modulation of N-type calcium channels by G-protein $\beta\gamma$ subunits. *Nature,* **380,** 255 – 258.

JONES, S.W. (1998). Overview of voltage-dependent calcium channels. *J. Bioenerg. Biomembr.,* **30,** 299 – 312.

KATO, M., YAMAGUCHI, H. & OCHI, R. (1990). Mechanism of adenosine-induced inhibition of calcium current in guinea pig ventricular cells. *Circ. Res.,* **67,** 1134 – 1141.

KING, B.F., TOWNSEND-NICHOLSON, A. & BURNSTOCK, G. (1998). Metabotropic receptors for ATP and UTP: exploring the correspondence between native and recombinant nucleotide receptors. *Trends Pharmacol. Sci.,* **19,** 506 – 514.

LIU, D.-M. & ADAMS, D.J. (2001). Ionic selectivity of native ATP-activated (P2X) receptor channels in dissociated neurones from rat parasympathetic ganglia. *J. Physiol.,* **534,** 423 – 435.

LUSTIG, K.D., SHIAU, A.K., BRAKE, A.J. & JULIUS, D. (1993). Expression cloning of an ATP receptor from mouse neuroblastoma cells. *Proc. Natl. Acad. Sci. U.S.A.,* **90,** 5113 – 5117.

MCMILLIAN, M.K., SOLTOFF, S.P., CANTLEY, L.C., RUDEL, R.A. & TALAMO, B.R. (1993). Two distinct cytosolic calcium responses to extracellular ATP in rat parotid acinar cells. *Br. J. Pharmacol.,* **108,** 451 – 461.

NOGUCHI, J. & YAMASHITA, H. (2000). Adenosine inhibits voltage-dependent Ca^{2+} currents in rat dissociated supraoptic neurones via A_1 receptors. *J. Physiol.,* **526,** 313 – 326.

QI, A.-D. & KWAN, Y.W. (1996). Modulation by extracellular ATP of L-type calcium channels in guinea-pig single sinoatrial nodal cell. *Br. J. Pharmacol.,* **119,** 1454 – 1462.

QIN, N., PLATANO, D., OLCESE, R., STEFANI, E. & BIRNBAUMER, L. (1997). Direct interaction of G $\beta\gamma$ with a C-terminal G $\beta\gamma$-binding domain of the Ca^{2+} channels α1 subunit is responsible for channel inhibition by G protein-coupled receptors. *Proc. Natl. Acad. Sci. U.S.A.,* **94,** 8866 – 8871.

RALEVIC, V. & BURNSTOCK, G. (1998). Receptors for purines and pyrimidines. *Pharmacol. Rev.,* **50,** 413 – 492.

RIBEIRO, J.A. (1996). Purinergic regulation of acetylcholine release. *Prog. Brain Res.,* **109,** 231 – 241.

ROBAYE, B., BOEYNAEMS, J.M. & COMMUNI, D. (1997). Slow desensitization of the human $P2Y_6$ receptor. *Eur. J. Pharmacol.,* **329,** 231 – 236.

SATHER, W.A., TANABE, T., ZHANG, J.-F., MORI, Y., ADAMS, M.E. & TSIEN, R.W. (1993). Distinctive biophysical and pharmacological properties of class A (BI) calcium channel α1-subunits. *Neuron,* **11,** 291 – 303.

SMITH, A.B., HANSEN, M.A., LIU, D.-M. & ADAMS, D.J. (2001). Pre- and postsynaptic actions of ATP on neurotransmission in rat submandibular ganglion. *Neuroscience,* **107,** 283 – 291.

SOONG, T.W., STEA, A., HODSON, C.D., DUBEL, S.J., VINCENT, S.R. & SNUTCH, T.P. (1993). Structure and functional expression of a member of the low voltage-activated calcium channel family. *Science,* **260,** 1133 – 1136.

STEA, A., DUBEL, S.J., PRAGNELL, M., LEONARD, J.P., CAMPBELL, K.P. & SNUTCH, T.P. (1993). A β-subunit normalizes the electrophysiological properties of a cloned N-type Ca^{2+} channels α1-subunit. *Neuropharmacology,* **32,** 1103 – 1116.

STEA, A., TOMLINSON, J.W., SOONG, T.W., BOURINET, E., DUBEL, S.J., VINCENT, S.R. & SNUTCH, T.P. (1994). Localization and functional properties of a rat brain α1A calcium channel reflect similarities to neuronal Q- and P-type channels. *Proc. Natl. Acad. Sci. U.S.A.,* **91,** 10576 – 10580.

SUZUKI, T., AIDA, H., AEBA, A. & SAKADA, S. (1990a). Responses of hamster submandibular ganglion cells to ATP. *Bull. Tokyo Dent. Coll.,* **31,** 63 – 65.

SUZUKI, T., FUKUDA, S. & SAKADA, S. (1990b). Adenosine hyperpolarization and slow hyperpolarizing synaptic potential in the hamster submandibular ganglion cell. *Bull. Tokyo Dent. Coll.,* **31,** 67 – 70.

TOMLINSON, W.J., STEA, A., BOURINET, E., CHARNET, P., NARGEOT, J. & SNUTCH, T.P. (1993). Functional properties of a neuronal class C L-type calcium channel. *Neuropharmacology,* **32,** 1117 – 1126.

VON KÜGELGEN, I., KURZ, K. & STARKE, K. (1993). Axon terminal P2-purinoceptors in feedback control of sympathetic transmitter release. *Neuroscience,* **56,** 263 – 267.

WELFORD, L.A., CUSACK, N.J. & HOURANI, S.M.O. (1986). ATP analogues and the guinea-pig taenia coli: a comparison of the structure – activity relationships of ectonucleotidases with those of the P_2-purinoceptor. *Eur. J. Pharmacol.,* **129,** 217 – 224.

WILLIAMS, M.E., BRUST, P.F., FELDMAN, D.H., PATTHI, S., SIMERSON, S., MAROUFI, A., MCCUE, A.F., VELICELEBI, G., ELLIS, S.B. & HARPOLD, M.M. (1992b). Structure and functional expression of an ω-conotoxin-sensitive human N-type calcium channel. *Science,* **257,** 389 – 395.

WILLIAMS, M.E., FELDMAN, D.H., MCCUE, A.F., BRENNER, R., VELICELEBI, G., ELLIS, S.B. & HARPOLD, M.M. (1992a). Structure and functional expression of α1, α2, and β subunits of a novel human neuronal calcium channel subtype. *Neuron,* **8,** 71 – 84.

YAMADA, E., ENDOH, T. & SUZUKI, T. (2002). Angiotensin II-induced inhibition of calcium currents via $G_{q/11}$-protein involving protein kinase C in hamster submandibular ganglion neurons. *Neurosci. Res.,* **43,** 179 – 189.

ZHONG, Y., DUNN, P.M. & BURNSTOCK, G. (2001). Multiple P2X receptors on guinea-pig pelvic ganglion neurons exhibit novel pharmacological properties. *Br. J. Pharmacol.,* **132,** 221 – 233.

ZIMMERMANN, H. (1994). Signaling via ATP in the nervous system. *Trends Neurosci.,* **17,** 420 – 426.

(Received November 14, 2002
Accepted March 3, 2003)